Journal of the European Ceramic Society xxx (xxxx) xxx–xxx

Contents lists available at ScienceDirect

Journal of the European Ceramic Society

journal homepage: www.elsevier.com/locate/jeurceramsoc

Original Article

Effect of NaF doping on the transparency, microstructure and spectral properties of Yb^{3+}: CaF_2 transparent ceramics

Weiwei Li[a], Wei Jing[b,*], Bingchu Mei[a,*], Pengfei Zhai[a], Yu Yang[a], Jinghong Song[c]

[a] State Key Laboratory of Advanced Technology for Materials Synthesis and Processing, Wuhan University of Technology, Wuhan, 430070, China
[b] Institute of Chemical Materials, China Academy of Engineering Physics, Mianyang, 621900, China
[c] Center of Materials Research and Analysis, Wuhan University of Technology, 122 Luoshi Road, Wuhan, 430070, China

ARTICLE INFO

Keywords:
Yb^{3+}: CaF_2
transparent ceramics
sintering aids
transmittance
spectroscopy modulation

ABSTRACT

Yb^{3+}:CaF_2 transparent ceramics are promising laser gain media with outstanding performance. However, low transmittance in the visible range is the main challenge that restricts the application of Yb^{3+}:CaF_2 ceramics in the laser system. In this paper, a new scheme to eliminate the residual pores in the Yb^{3+}:CaF_2 transparent ceramics based on doping of NaF as a sintering aid is proposed. Microstructural characterization indicated that NaF could inhibit the grain growth and increase the transmittance in the visible range significantly. The corresponding transmittance was measured to be 85% at the wavelength of 400 nm. The spectra results showed that co-doped with Na^+ ions could break the clusters of Yb^{3+} ions and modulate the spectroscopy properties of Yb^{3+}: CaF_2 lattice efficiently. This paper proved that doping with NaF is an efficient strategy to improve the transmittance and fluorescence quantum efficiency of Yb^{3+}:CaF_2 transparent ceramics.

1. Introduction

Yb^{3+} doped materials with high quantum efficiency have been investigated widely in the last decades for the following reasons : (1) Yb^{3+} ions have a simple energy level, effects such as excited state absorption, cross-relaxation, up-conversion and concentrations quenching are absent from Yb^{3+} ions [1]. (2) Yb^{3+} ions as the active ions have strong absorption and emission cross sections, particularly the strong absorption around 980 nm, which is very well suited for pumping by high-power InGaAs diodes for high power [2,3]and ultra-fast femtosecond lasers system [4]. In the past years, many Yb^{3+}doped materials for the laser system have been reported, but most of them have been focused on oxide materials, such as $Y_3Al_5O_{12}$ (YAG) [5,6], $Y_3Sc_2Al_3O_{12}$ (YSAG) [7],Y_2O_3 [8], Lu_2O_3 [9], Sc_2O_3 [10] and $Lu_3Al_5O_{12}$ (LuAG) [11], only a few works have been carried out on Yb^{3+}doped fluorides, e.g. YLF[12], KYF[13], SrF_2[14,15] and so on.

Compared to the oxides, fluorides have several advantages, such as broad transmission region (0.2-9 μm), lower refractive-index-limiting and nonlinear effect, low phonon energy, which prevents the impact of multi-phonon relaxation in electronic levels of impurity ions and introduced high amounts of active ions easily. Among the fluoride-based materials, CaF_2 has high thermal conductivity (10 W/mK), moisture resistance and cubic structure. The cubic structure makes it possible for fabrication CaF_2 polycrystalline transparent ceramics because non-cubic materials usually have multiple indices of refraction. Therefore, the birefringence effects in the randomly oriented grains of the anisotropic materials lead to the opaque [16–18].

Recently, Yb^{3+}: CaF_2 transparent ceramics have attracted great attention because of their intrinsic characterizations: such as low fabrication cost, high concentration and uniform dispersion of activated ions. In 2009, Yb^{3+}: CaF_2 transparent ceramics were obtained by a hot-pressed (HP) method, but the optical quality was not high [19]. Then, the first laser generation was demonstrated in 3 at.% Yb: CaF_2 ceramics in 2013[20]. Although excellent laser performance has been obtained for Yb^{3+}: CaF_2[21,22] and Yb^{3+}: CaF_2-LaF_3[23] transparent ceramics recently, scattering coefficient at short wavelength is still high at present that restricts the laser output power. How to improve the transmittance in the visible range is the main challenge at present. Considering the successful fabrication of YAG laser ceramics with the sintering aid of the SiO_2[24–26], it was obvious interest to examine the effect of sintering aids on the fabrication of Yb^{3+}: CaF_2 transparent ceramics.

The melting point of CaF_2 (1423℃) is lower than that of YAG (1950℃), it is more suitable to consider the sintering aids with low melting point such as NaF (993 ℃). In addition, it is easy to form cluster structure when trivalent Yb^{3+} doped in CaF_2 host even in low doping concentrations [27], which degrade the luminescent properties and quantum efficiency. Na^+ substitutes Ca^{2+}, so the pair Yb^{3+}/Na^+ is

* Corresponding author.
E-mail addresses: jingwei@caep.cn (W. Jing), bcmeilab@163.com (B. Mei).

https://doi.org/10.1016/j.jeurceramsoc.2020.06.001
Received 2 April 2020; Received in revised form 20 May 2020; Accepted 1 June 2020

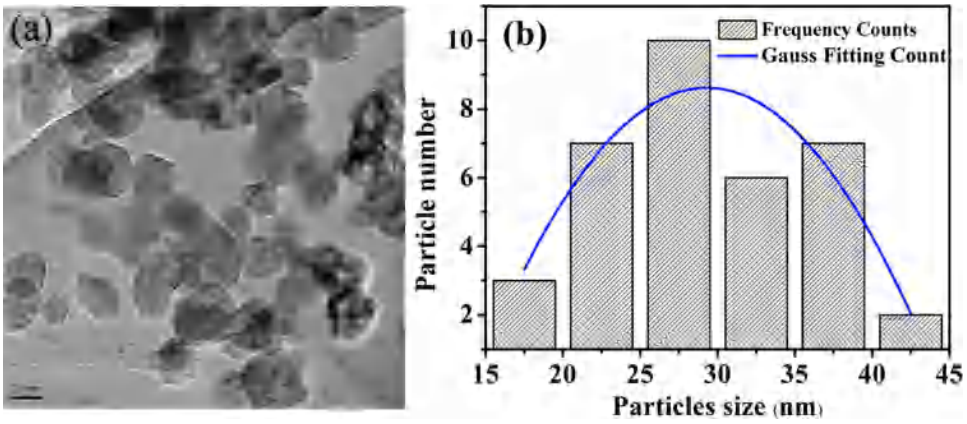

Fig. 1. (a) TEM image and (b) the size distribution of Yb^{3+} dope CaF_2 nanoparticles.

charge balanced for the substituted Ca^{2+}/Ca^{2+} pair. Formation of interstitial F^- should be prevented by the charge compensation [28,29]. Besides, the laser pumping threshold power of Yb^{3+} doped CaF_2 single crystal is relatively high due to operating in a quasi-three-level energy laser system. Yb^{3+}-Na^+ co-doped CaF_2 single crystal could operate in a relatively low threshold pump power and achieve highly efficient self-Q-switching performance [30]. But whether NaF has the same mechanism and effect in Yb^{3+}: CaF_2 transparent ceramics should be required further investigation.

In this paper, 5 at.% Yb^{3+}-doped and Yb^{3+}, Na^+ co-doped CaF_2 transparent ceramic with different weight of NaF (0.5 wt.%, 1 wt.%, 5 wt.% and 10 wt.%) have been prepared by hot-pressed (HP) method for the first time. The purpose of this paper was to investigate the influence of Na^+ on the transparency, microstructure and spectral properties of Yb^{3+}: CaF_2 transparent ceramics.

2. Experimental

2.1. Ceramics preparation

5 at.% Yb^{3+}: CaF_2 powders were synthesized by co-precipitation method according to our previous report [31]. The process of particles synthesis can be described as follows: aqueous solutions of Ca $(NO_3)_2{\cdot}4H_2O$ (99.0%, Sinopharm), $Yb(NO_3)_3{\cdot}5H_2O$ (99.99%, Alfa Aesar), $KF{\cdot}2H_2O$ (99.0%, Sinopharm), and NaF (99.9%, Sinopharm) served as the starting compounds. First, 30.23 g $Ca(NO_3)_2$ and 26.55 g KF were dissolved in 64 ml deionized water in beaker, respective. Then 1.845 g $Yb(NO_3)_3$ was poured-in $Ca(NO_3)_2$ aqueous solution, the mixture was stirred magnetically until it was homogeneous. Second, the KF solution was dropped wise to the solution of $Ca(NO_3)_2{\cdot}4H_2O$ and Yb $(NO_3)_3{\cdot}5H_2O$ under magnetic stirring and stirred a few minutes until the reaction process completed. The precipitation was centrifuged to separate from the water, and then washed by deionized water few times. The precipitation was put into the dry oven and maintained at 80 °C for 24 h. After cooling to room temperature, the white solid was repeatedly ground for 30 min.

In order to introduce the Na^+ to the CaF_2 lattice, NaF was added to Yb^{3+}: CaF_2 powders in an agate mortar containing 20 ml ethanol according to the stoichiometric ratio. Milled 30 min to make mixing uniformity and then put it in a dry oven for 12 h in 80 °C. Yb^{3+}: CaF_2 powders doped with different concentrations of 0, 0.5, 1, 5 and 10 wt.% (calculated on the 5 at.% Yb^{3+}: CaF_2 powder mass) were prepared following the same process. 2.3 g Yb^{3+}: CaF_2/NaF mixed powders were loaded into a 16-mm-diameter graphite mold and sintered by the hot-pressed method. The heating rate was 15 °C/min from room temperature to 800 °C and the vacuum was maintained during the whole sintering process. The ultimate sample was 16 mm in diameter and 2 mm in thickness. Finally, both surfaces of the samples were polished using diamond slurries.

2.2. Characterization

Particle size and morphology were investigated by transmission electron microscope (JEOL JEM 2100 F, Japan). The thermoanalysis of Yb^{3+}: CaF_2 powders was measured on a thermal analyzer (STA449C/3/G, Netzsch) (10k/min, N_2). The phase of the samples was identified by the X-ray diffraction(Japan, Rigaku, D/Max-RB). The surface morphology (grain boundary and pores) of the sintered ceramics was obtained in U8010 FSEM. The transmission and absorption spectra were measured on the UV-3600 (Shimadzu). The luminescent spectrum and the fluorescence decay curves were performed on a FLS1000 spectrofluorometer (Edinburgh). All the samples were polished into 0.5 mm to decreased the reabsorption effect when measured the emission spectral and the lifetime. The slit width of the excitation and emission sides of FLS1000 spectrofluorometer were settled at the same condition to compare the effect of NaF on the spectra properties of Yb^{3+}: CaF_2 ceramics.

3. Results and discussion

The particle morphology and size distribution of 5 at.% Yb^{3+}: CaF_2 nanoparticles was shown in Fig. 1. The figure indicated that the synthesized 5 at.% Yb^{3+}: CaF_2 nanoparticles exhibited the spherical-like morphology. Using the Image-Pro Plus 6.0 software, the average particle size of the Yb^{3+}: CaF_2 powders from Gaussian fitting of the histogram (see Fig. 1 (b)) was found to be about 29 ± 1 nm.

Fig. 2 shows the differential scanning calorimetry and thermogravimetric analysis (DSC-TG) curves of 5 at.% Yb^{3+}: CaF_2 powders synthesized by co-precipitation in distilled water. The measuring

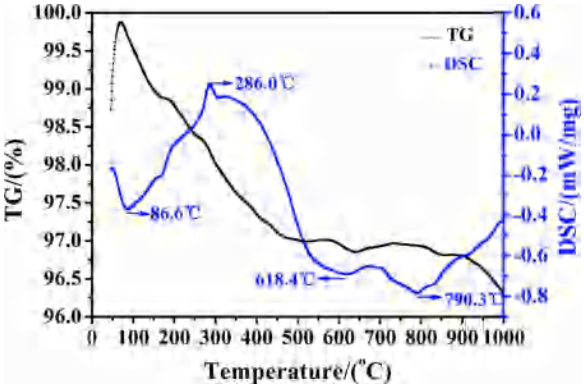

Fig. 2. DSC-TG curves of 5 at.% Yb^{3+}: CaF_2 powders.

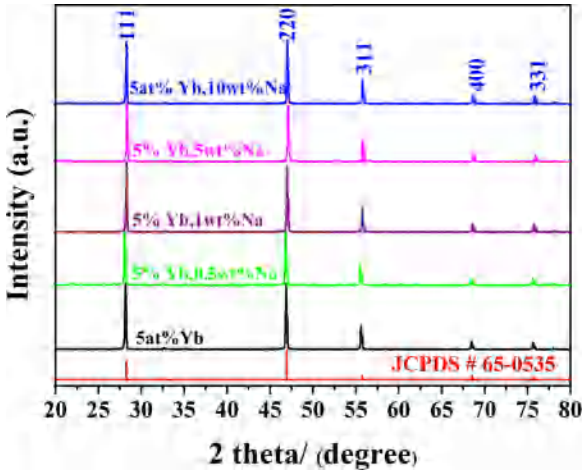

Fig. 3. X-ray diffraction of Yb^{3+}: CaF_2 transparent ceramics co-doped with different concentration Na^+ ions.

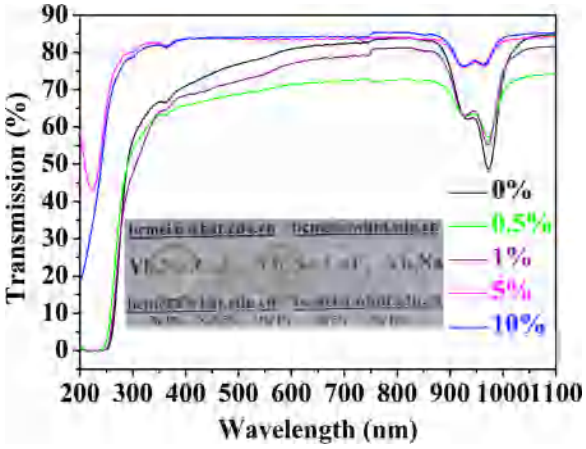

Fig. 4. In-line transmittance of the 5 at. % Yb^{3+}: CaF_2 transparent ceramics with different concentration of NaF. The inset shows the photo of the obtained samples.

temperature ranged from 45 °C to 1000 °C with a heating rate of 10 °C/min. The TG curve indicates two major drops between 20 °C-580 °C and 580 °C-800 °C that the total weight loss was about 2.83%. Because the powder was synthesis by the wet-chemical route, abundant adsorbed ions would absorb in the nano-particles surface. The residual adsorbed ions such as OH^- and NO_3^- ions decomposed when the powders were heated. So, the change of weight can be ascribed to the loss of the residual adsorbed ions. There was one exothermic peak appeared at 286 °C in the DSC curve, which was corresponding to the decomposition of OH^- and NO_3^- ions. Three endothermic peaks around 86.6 °C, 618 °C and 790.3 °C were observed, the peak at the temperature of 86.6 °C was attributed to the evaporation of free water absorbed from the particles and the peak at 618 °C was due to the removal of organic materials. The endothermic peaks at 790.3 °C might be the ultimate point of densification.

The XRD patterns of different concentration of Na^+ ions co-doped Yb^{3+}: CaF_2 transparent ceramics sintered at 800 °C combined with data from JCPDS card # 65-0535 for CaF_2 are shown in Fig. 3. It can be clearly seen that all the peaks can be indexed in the CaF_2 cubic phase of the fluorite-type structure (space group: Fm3m). The phase and structure of the ceramics did not change even the Na^+ ions concentration reached to 10 wt.%. No other phases referred to Na^+ or Yb^{3+} ions were detected in all the XRD patterns, suggesting that Na^+ and Yb^{3+} ions successfully incorporated into the CaF_2 structure and occupied the sites of Ca^{2+} ions. Calculated from the XRD data, the lattice parameters of 5at.% Yb^{3+}: CaF_2 ceramics with different concentrations of 0, 0.5, 1, 5 and 10 wt.% were about 5.4851, 5.4781, 5.4616, 5.4605 and 5.4544 Å, respectively. It could be clearly seen that the lattice constant decreased with the increasing of NaF content, a possible explanation is that the discrepancy of ionic radii between Na^+(0.102 Å), Yb^{3+}(0.868 Å) and Ca^{2+} (0.100 Å), resulting in a shrinkage of the unit cell volume when Yb^{3+}-Na^+ replace Ca^{2+}- Ca^{2+} ions pairs.

All the samples were polished to 2 mm thickness for the optical properties test. Fig. 4 shows the in-line transmittance and photo of Yb^{3+}: CaF_2 transparent ceramics with different concentration of NaF sintered at 800 °C for 2 h. It could be seen that the all the sintered Yb^{3+}: CaF_2 ceramics were highly transparent and the words on the printed paper could be clearly seen. For the sample without NaF doping, the transmittance at the wavelength of 1200 nm and 400 nm were about 84% and 70%, respectively. The poor surface roughness of the Yb^{3+}: CaF_2 ceramics was responded for the low transmittance that laser-level polishing process would be introduced in the further work. Due to the residual nano-size pores in the ceramics, the transmittance of the 5 at. % Yb^{3+}: CaF_2 with 0, 0.5 and 1 wt.% NaF decrease with the decreasing of wavelength according to the Rayleigh' equation [32]· However, the transmittance in the short-wavelength hardly decreased when the NaF concentration was increased to 5 wt.%. The transmittance in the wavelength of 1200 nm and 400 nm were 85% and 83%, respectively. However, when NaF concentration further increased to 10 wt.%, the measured transmittance rarely increased anymore compared with the 5 wt.% doped sample. Considering the transmittance results, it could be inferred that doped with NaF could increase the transmittance in the visible range significantly under the same sintering process and the optimal addition of NaF in Yb^{3+}: CaF_2 transparent ceramics might be about 5 wt.%.

To find out the reason of the increased transmittance at 400 nm, the FSEM microstructure of ceramics is shown in Fig. 5. Both the undoped and NaF doped samples presented a full dense microstructure and no pores or other phases were detected. The average grain size was calculated by the linear intercept method [33]. It could be clearly seen that the average grain size of 5 wt.% NaF doped Yb^{3+}: CaF_2 sample is smaller than the sample without NaF doping. The average grain size of the undoped and 5 wt.% NaF doped Yb^{3+}: CaF_2 sample is about 445 ± 8 nm and 120 ± 3 nm, respectively. The grain growth of the NaF doped Yb^{3+}: CaF_2 sample is quite limited compared with the initial particle size of the Yb^{3+}: CaF_2 nanopowders (about 29 nm). The grain size of the NaF doped Yb^{3+}: CaF_2 sample is even smaller than the grain size of ceramics fabricated by SPS method [34]. From the dislocation theory, the grain boundary is the obstacle of dislocation movement. Small grain size could provide more grain boundaries to prevent the dislocation and improve the mechanical properties of ceramics according to the Hall-Petch equation. It is gratifying that Yb^{3+}: CaF_2 transparent ceramics fabricated by HP method presented small grain size, which is beneficial to the mechanical properties' improvement and thus can achieve higher power laser output under the same optical quality.

The function of NaF additive is shown in two aspects: First, doping with NaF in CaF_2 powders reduces the migration rate and provide sufficient time for the pore removal, so that the sample could be sintered at a relatively uniform densification rate. At the same time, NaF inhibited the grain boundaries moving and grain growth. The small grains mean more boundaries, which provide more channels for pores elimination and enhanced the transmittance value of short wavelength.

The room temperature absorption spectra of the 5 at.% Yb^{3+}: CaF_2 transparent ceramics without NaF doping and different contents of NaF doped in the wavelength range of 800-1100 nm are shown in Fig. 6. There were two absorption peaks located at 926 nm and 973 nm, corresponding to the transition between ground level $^2F_{7/2}$ to the excited level $^2F_{5/2}$ of Yb^{3+} ion. It is clearly seen that absorption intensity decreased with the increase of NaF content because the transition

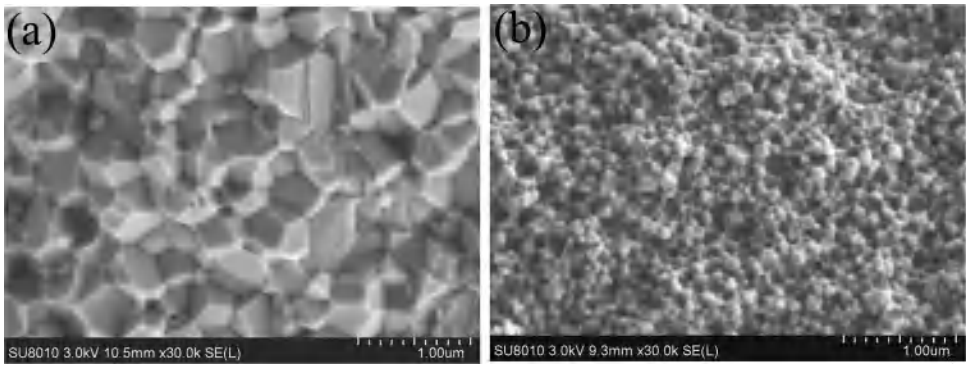

Fig. 5. FSEM images of (a) undoped and (b) NaF doped Yb^{3+}: CaF_2 samples.

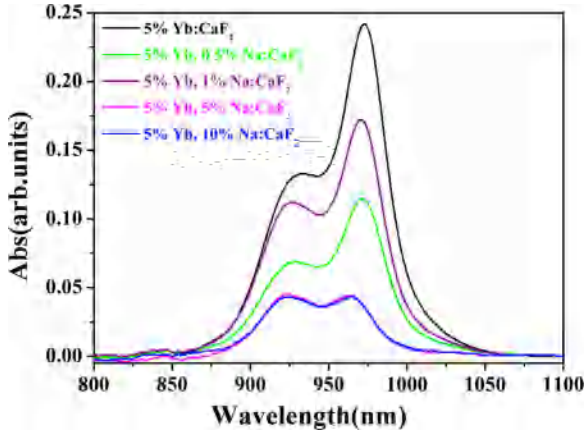

Fig. 6. Absorption spectra of Yb^{3+}: CaF_2 ceramics.

oscillator strength of Yb-Na ion pairs formed in the high concentration of NaF doped Yb^{3+}: CaF_2 sample, which is lower than that Yb-F ion pair. As a consequence, the absorption intensity decreased after doped with NaF in the Yb^{3+}: CaF_2 samples. When the power of pump source is constant, clearly the decreased absorption intensity is unfavorable for absorbing the pump energy. This means that higher concentration of active ions or larger size of the samples are needed to achieve the corresponding absorption efficiency.

Fig. 7 shows the emission spectra of undoped and different contents

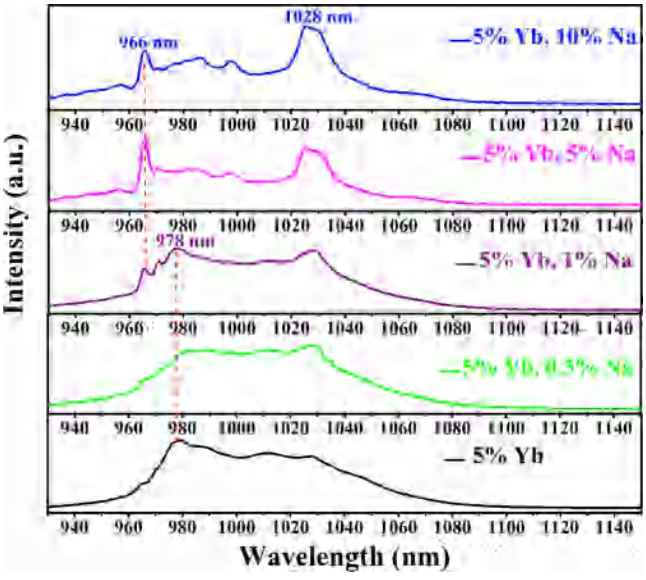

Fig. 7. Emission spectra of Yb^{3+}: CaF_2 ceramics under 896 nm excitation.

of NaF doped 5 at.% Yb^{3+}: CaF_2 transparent ceramics under the excitation of 896 nm recorded at room temperature. It can be observed that the strongest emission peak of the undoped Yb^{3+}: CaF_2 sample located at 978 nm, which was the characteristic zero phonon emission of Yb^{3+} ions. After codoped with 0.5 wt.% NaF, the emission spectrum is different from the undoped-NaF sample that the strong emission changed to the laser emission peak of 1028 nm and the emission intensity at 1028 nm was increased gradually. Besides, the emission peak of NaF doped Yb^{3+}: CaF_2 samples at 1028 nm presented a very broad bandwidth, which was promising beneficial to realize tunable laser and ultra-short laser pulses. This result was also reported by L. B. Su et al. [28] in Yb, Na: CaF_2 single crystal that followed the same trend. Trivalent Yb^{3+} ions easily form cluster structure in CaF_2 even in low doping concentrations, the clusters were the dominated structure in 5 at. % Yb: CaF_2 sample. Therefore, the low emission intensity at 1028 nm was caused by the fluorescence quenching due to cooperative luminescence between Yb-Yb ion pairs. After doped with NaF, Na^+ ions replaced the Ca^{2+} ion in the nearest neighbor of Yb^{3+} ions and the formed Yb-Na ions pairs prevent the Yb^{3+} ions form the Yb-Yb clusters. The eventual result is that the emission intensity at 1028 nm was enhanced gradually with the increasing doping concentration of NaF. In addition, when doped with 1 wt.% NaF, the intensity of emission peak at 966 nm was increased and the emission peak at 976 nm disappeared, especially at high doping concentration. In fact, the appearance of this emission peak is a signature of forming an isolated cubic (O_h) luminescent center in the CaF_2 [35]. It also proved that introduced NaF could break the cluster structure of Yb^{3+} ion in CaF_2 host.

Fig. 8 shows the decay curves of the emission at 1028 nm for 5 at.% Yb^{3+}: CaF_2 transparent ceramics with different content of NaF. The decay time curves for all the ceramics were fitted with a single-exponential function.

$$I(t) = A + Be^{-\frac{t}{\tau}}$$

Where A and B are fitting constants, t is the decay time and τ is the lifetime. The lifetimes were estimated to be 3.75 ms, 3.84 ms, 4.28 ms, 6.43 ms and 8.15 ms for 0, 0.5 wt.%, 1 wt.%, 5 wt.% and 10 wt.% doped Yb^{3+}: CaF_2 ceramics, respectively. Significantly, the lifetime increased with the increasing of Y^{3+} ions concentration, which was in good accordance with the result of the luminesce intensity. The increased lifetime was due to the higher quantum efficiency that benefited from breaking the cluster structure of Yb^{3+} ions. The lifetime of 8.15 ms of 10 wt.% doped Yb^{3+}: CaF_2 ceramics is close to the value of 0.1 at.% Yb^{3+}: CaF_2 single crystal [27], which is believed to be no cluster structure in such low Yb^{3+} doping concentration. Fluorescence lifetime represents the energy storage capacity, longer lifetime would help to obtain populationinversion easier and achieve higher power laser output.

From the result of the absorption spectra, it can be clearly seen that doping with NaF reduces the absorption intensity of the Yb^{3+}: CaF_2 samples, but increased the emission intensity and fluorescence lifetime.

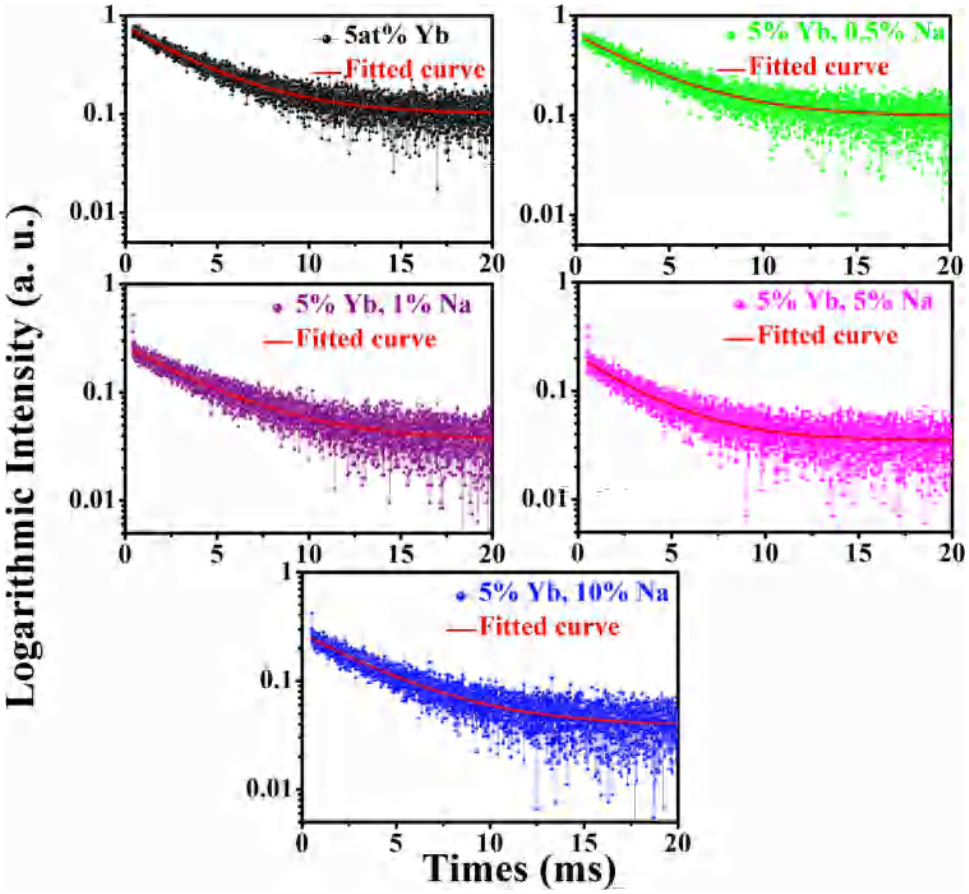

Fig. 8. Decay curves of Yb^{3+}: CaF_2 ceramics under 896 nm excitation.

The influence of NaF doping on the laser performance of the ceramics needs further investigation, this part of work is in progress and will be discussed in a forthcoming paper.

4. Conclusions

This paper discussed the effect of NaF on the transparency, microstructure and spectra properties of Yb^{3+}: CaF_2 transparent ceramics fabricated by HP method. The presence of NaF plays two roles in Yb^{3+}: CaF_2 ceramics: first, as sintering aids, NaF inhibited the grain growth and increased the transmittance in the visible wavelength significantly. The transmittance of the LiF doped samples reached to 83% and 85% at the wavelength of 400 nm and 1200 nm, respectively. Second, doped with NaF prevented Yb^{3+} ions forming cluster structure in Yb^{3+}: CaF_2 ceramics. The emission intensity of 1028 nm and the luminescence lifetime increased with the increase of NaF doping concentration. Therefore, this paper suggested that doping with NaF is an effective method to improve the transmittance in the short-wavelength and fluorescence quantum efficiency of Yb^{3+}: CaF_2 transparent ceramics.

Declaration of Competing Interest

The authors declare that they have no known competing financial interests or personal relationships that could have appeared to influence the work reported in this paper.

Acknowledgments

This work was supported by the National Natural Science Foundation of China (Grant No. 51902234 and 51972245), Fundamental Research Funds for the Central Universities (Grant No. WUT: 2019IVA065, 2020IVB003 and 2019-YB-011) and the State Key Laboratory of Advanced Technology for Materials Synthesis and Processing (Wuhan University of Technology) (Grant No. 2020-KF-16).

References

[1] G. Boulon, Why so deep research on Yb^{3+}-doped optical inorganic materials, J. Alloy Compd. 451 (2008) 1–11.
[2] M. Siebold, M. Hornung, R. Boedefeld, S. Podleska, S. Klingebiel, C. Wandt, F. Krausz, S. Karsch, R. Uecker, A. Jochamnn, J. Hein, M.C. Kaluza, Terawatt diode-pumped Yb: CaF_2 laser, Opt. Lett. 33 (2008) 2770–2772.
[3] S. Ricaud, D.N. Papadopoulos, A. Pellegrina, F. Balembois, P. Georges, A. Courjaud, P. Camy, J.L. Doualan, R. Moncorge, F. Druon, High-power diode-pumped cryogenically cooled Yb: CaF_2 laser with extremely low quantum defect, Opt. Lett. 36 (2011) 1602–1604.
[4] A. Lucca, G. Debourg, M. Jacquement, F. Druon, F. Balembois, P. Georges, High power diode-pumped Yb^{3+}: CaF_2 femtosecond laser, Opt. Lett. 29 (2004) 2767–2769.
[5] N. Jiang, C. Ouynag, Y. Liu, W.X. Li, Y.L. Fu, T.F. Xie, Q. Liu, Y.B. Pan, J. Li, Effect of air annealing on the optical properties and laser performance of Yb: YAG transparent ceramics, Opt. Mater. 95 (2019) 109203.
[6] S.Q. Yu, W. Jing, M.J. Tang, T. Xu, W.L. Yin, B. Kang, Fabrication, microstructure and optical properties of large-sized Nd: YAG and composite Yb: YAG transparent ceramic slabs, Ceram. Int. 45 (2019) 19340–19344.
[7] M.S. Nikova, V.A. Tarala, D.S. Vakalov, D.S. Kuleshov, A.A. Kravtsov, S.V. Kuznetsov, I.S. Chikulina, F.F. Malyavin, L.V. Tarala, E.A. Evtushenko, V.A. Lapin, M.A. Pankov, Temperature-related changes in the structure of YSAG: Yb garnet solid solutions with high Sc^{3+} concentration, J. Eur. Ceram. Soc. 39 (2019) 4946–4956.
[8] J. Wang, D.L. Yin, J. Ma, P. Liu, Y. Wang, Z.L. Dong, L.B. Kong, D.Y. Tang, Pump Laser induced photodarkening in ZrO_2-doped Yb: Y_2O_3 laser ceramics, J. Eur. Ceram. Soc. 39 (2019) 635–640.
[9] L.L. Dong, M.Z. Ma, W. Jing, T. Xu, K. Bin, R.S. Guo, Synthesis and highly sinterable Yb: Lu_2O_3 nanopowders via spray co-precipitation for transparent ceramics, Ceram. Int. 45 (2019) 19554–19561.
[10] G. Toci, J. Hostasa, B. Patrizi, V. Biasini, A. Pirri, A. Piancastelli, M. Vannini, Fabrication and laser performances of Yb: Sc_2O_3 transparent ceramics from different combination of vacuum sintering and hot isostatic pressing conditions, J. Eur. Ceram. Soc. 40 (2020) 881–886.

[11] L. Basyrova, R. Maksimov, V. Shitov, M. Baranov, V. Mikhaylovsky, A. Khubetsov, O. Dymshits, X. Mateos, P. Loiko, Effect of SiO_2 addition on structural and optical properties of Yb: $Lu_3Al_5O_{12}$ transparent ceramics based on laser ablated nano-powders, J. Alloy Compd. 806 (2019) 717–725.

[12] U. Demirbas, J. Thesinga, H. Cankaya, M. Kellert, F.X. Kartner, M. Pergament, High-power passively mode-locked cryogenic Yb: YLF laser, Opt. Lett. 45 (2020) 2050–2053.

[13] A. Volpi, G. Cittadino, A. Di Lieto, M. Tonelli, Anti-Stokes cooling of Yb-doped KYF_4 single crystals, J. Lumin. 203 (2018) 670–675.

[14] Z.T. Zou, Y.F. He, H. Yu, S.Y. Pang, Y.J. Wu, J. Liu, L.B. Su, Photoluminescence property and laser performance in Yb-doped $Sr_{1-x}Gd_xF_{2+x}$ single crystals, Opt. Mater. Express 8 (2018) 1747–1753.

[15] W.W. Li, H.J. Huang, B.C. Mei, J.H. Song, Synthesis of highly sinterable Yb: SrF_2 nanopowders for transparent ceramics, Opt. Mat. 75 (2018) 7–12.

[16] D.J. Winsniewski, L.A. Boatner, J.S. Neal, G.E. Jellison, J.O. Ramey, A. Northe, M. Wisniewska, A.E. Payzant, J.Y. Howe, A. Lempicki, C. Brecher, J. Glodo, Development of novel polycrystalline ceramic scintillators, IEEE T. Nucl. Sci. 55 (2008) 1501–1508.

[17] S. Chen, Y.Q. Wu, Y. Yang, Spark plasma sintering of hexagonal structure Yb^{3+}-doped $Sr_5(PO_4)_3F$ transparent ceramics, J. Am. Ceram. Soc. 96 (2013) 1694–1697.

[18] Y.Q. Wu, Nanostructured transparent ceramics with an anisotropic crystalline structure, Opt. Mater. Express 4 (2014) 2026–2031.

[19] P. Aubry, A. Bensalah, P. Gredin, G. Patriarche, D. Vivien, M. Moriter, Synthesis and characterizations of Yb-doped CaF_2 ceramics, Opt. Mater. 31 (2009) 750–753.

[20] M. Sh. Akchurin, T.T. Basiev, A.A. Demidenko, M.E. Doroshenko, P.P. Fedorov, E.A. Garibin, P.E. Gusev Kuznetsov, M.A. Krutov, I.A. Mironov, V.V. Osiko, P.A. Popov, CaF_2: Yb laser ceramics, Opt. Mater. 35 (2013) 444–450.

[21] P. Aballea, A. Suganuma, F. Druon, J. Hostalrich, P. Georges, P. Gredin, M. Moriter, Laser performance of diode-pumped Yb: CaF_2 optical ceramics synthesized using an energy-efficient process, Optica 2 (2015) 288–291.

[22] J. Sarthou, P. Aballea, G. Patriarche, H. Serier-Brault, A. Suganuma, P. Gredin, M. Mortier, Wet-route synthesis and characterization of Yb: CaF_2 optical ceramics, J. Am. Ceram. Soc. 99 (2016) 1992–2000.

[23] S. Kitajima, K. Yamakado, A. Shirakawa, K.I. Ueda, Y. Ezura, H. Ishizawa, Yb^{3+}-doped CaF_2-LaF_3 ceramics laser, Opt. Lett. 42 (2017) 1724–1727.

[24] Y.K. Li, S.M. Zhou, H. Lin, X.R. Hou, W.J. Li, H. Teng, T.T. Jia, Fabrication of Nd: YAG transparent ceramics with TEOS, MgO and compound additives as sintering aids, J. Alloy Compd. 502 (2010) 225–230.

[25] H. Yang, X.P. Qin, J. Zhang, J. Ma, D.Y. Tang, S.W. Wang, Q.T. Zhang, The effect of MgO and SiO_2 codoping on the properties of Nd: YAG transparent ceramic, Opt. Mater. 34 (2012) 940–943.

[26] S. Kochawattana, A. Stevenson, S.-H. Lee, M. Ramirez, V. Gopalan, J. Dumm, V.K. Castillo, G.J. Quarles, G.L. Messing, Sintering and grain growth in SiO_2 doped Nd: YAG, J. Eur. Ceram. Soc. 28 (2008) 1527–1534.

[27] V. Petit, P. Camy, J.-L. Doualan, X. Portier, R. Moncorge, Spectroscopy of Yb^{3+}: CaF_2: From isolated centers to clusters, Phys. Rev. B 78 (2008) 085131.

[28] L.B. Su, J. Xu, H.J. Li, W.Q. Yang, Z.W. Zhao, J.L. Si, Y.J. Dong, G.Q. Zhou, Codoping Na^+ to modulate the spectroscopy and photoluminescence properties of Yb^{3+} ion CaF_2 laser crystal, Opt. Lett. 30 (2005) 1003–1005.

[29] L.B. Su, J. Xu, H.J. Li, L. Wen, Y.Q. Zhu, Z.W. Zhao, Y.J. Dong, G.Q. Zhou, J.L. Si, Sites structure and spectroscopic properties of Yb-doped and Yb, Na-codoped CaF_2 laser crystals, Chem. Phys. Lett. 406 (2005) 254–258.

[30] L.B. Su, J. Xu, Y. Hong Xue, C.Y. Wang, L. Chai, X.D. Xu, G.J. Zhao, Low-threshold diode-pumped Yb^{3+}, Na^+: CaF_2 self-Q-switched laser, Opt. Express 13 (2005) 5635–5640.

[31] W.W. Li, H.J. Huang, B.C. Mei, J.H. Song, X.D. Xu, Effect of Y^{3+} ion doping on the microstructure, transmittance and thermal properties of CaF_2 transparent ceramics, J. Alloy Compd. 747 (2018) 359–365.

[32] A. Ikesue, K. Kamata, T. Yamamoto, I. Yamaga, Optical scattering centers in polycrystalline Nd: YAG laser, J. Am. Ceram. Soc. 80 (1997) 1517–1522.

[33] M.I. Mendelson, Average grain size in polycrystalline ceramics, J. Am. Ceram. Soc. 52 (1969) 443–446.

[34] W.W. Li, B.C. Mei, J.H. Song, W.B. Zhu, G.Q. Yi, Yb^{3+} doped CaF_2 transparent ceramics by spark plasma sintering, J. Alloy Compd. 660 (2016) 370–374.

[35] T. Kallel, M.A. Hassairi, M. Dammak, A. Lyberis, P. Gredin, M. Mortier, Spectra and energy levels of Yb^{3+} ions in CaF_2 transparent ceramics, J. Alloy Compd. 584 (2014) 261–268.